PHYSICAL REVIEW D VOLUME 43, NUMBER 1 1 JANUARY 1991

Chiral symmetry and the large-N_c limit in K_{l4} decays

C. Riggenbach and J. Gasser
Institut für Theoretische Physik, Universität Bern, CH-3012 Bern, Switzerland

John F. Donoghue*
CERN, Geneva, Switzerland

Barry R. Holstein
Department of Physics and Astronomy, University of Massachusetts, Amherst, Massachusetts 01003
(Received 31 July 1990)

The treatment of kaon decays using chiral symmetry yields predictions for the form factors in $K \to \pi\pi e\nu$. In addition, the large-N_c limit of QCD implies that a particular combination of low-energy constants should be suppressed. We present the chiral predictions for K_{l4} decays at next-to-leading order in the energy expansion. By combining the phenomenologies of K_{l4} and $\pi\pi$ scattering, we test these predictions and provide a determination of the parameters in the chiral Lagrangian of QCD.

I. INTRODUCTION

In this paper we describe the analysis of the reactions labeled (Refs. 1–4) K_{l4}, that is

$$K \to \pi\pi l\nu ,$$

where $l = e,\mu$. While at first sight this would seem simply one of many kaon decay modes, it in fact has some special significance in the theory of chiral symmetry.[5–7] It is the simplest process which can test predictions which follow in the limit of large numbers of colors (large N_c).[7(a),8] The theory of chiral symmetry allows the description of the couplings of kaons and pions using a set of nonlinear Lagrangians, with coefficients which are to be determined phenomenologically. However, in the large-N_c limit, certain linear combinations of these coefficients are suppressed, as they correspond to extra quark loops. An illustration of allowed and disallowed diagrams for the K_{l4} process is given in Fig. 1. Although similar diagrams could be drawn for pionic processes, such as $\pi\pi$ scattering, the constraints of chiral symmetry are such that these diagrams cannot be disentangled using reactions which involve only pions, and one must consider kaonic reactions in order to perform the separation. The scattering of $K\pi$ or $K\bar{K}$ could in principle be used, but these reactions are poorly known and occur at too high an energy to be useful. The only purely phenomenological constraint on the large-N_c predictions of which we are aware comes from K_{l4} decay. It is therefore worthwhile to provide as complete an analysis as possible of this reaction in order to both explore the limits on the large-N_c result and to provide additional input to the chiral Lagrangian.

The predictions for the K_{l4} form factors at lowest order (i.e., order E^2) in the energy expansion of chiral symmetry were first given by Weinberg.[9] The experimental results are 30–50 % above the lowest-order predictions. The required additional contributions must come from higher orders in the energy expansion. We provide this next-order treatment by including loop diagrams as well as tree-level effects from the order-E^4 chiral Lagrangian. The latter are parametrized by a small number of low-energy constants. However, only three of these play a significant role. Two of these low-energy constants ap-

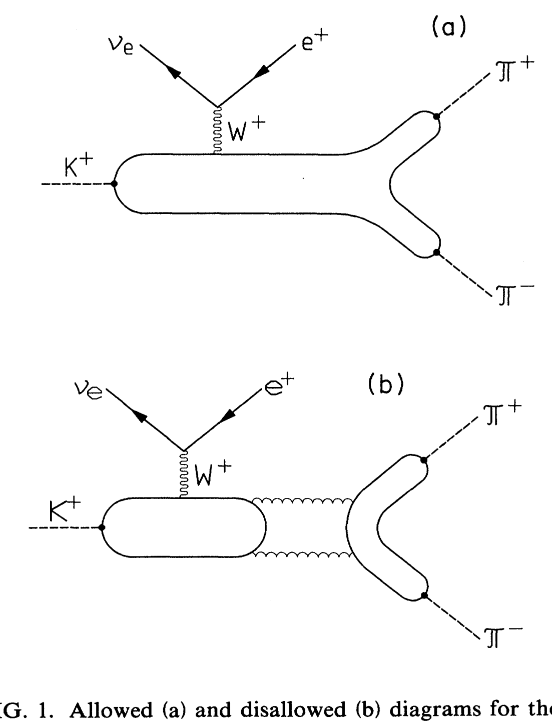

FIG. 1. Allowed (a) and disallowed (b) diagrams for the K_{l4} process at large N_c. Dashed lines denote axial-vector currents; wavy lines: gluon exchange.

pear in the analysis of $\pi\pi$ scattering. The third is first seen in K_{l4} decay. One combination of these low-energy constants is predicted to be suppressed at $N_c \to \infty$. A result of our analysis will be that a small nonzero value for this combination is favored phenomenologically, but with experimental errors which allow it to vanish at the 1 standard deviation level. Overall a good description of K_{l4} decays and $\pi\pi$ scattering is obtained.

The plan of the paper is as follows. In Sec. II, we define the form factors and review the experimental results. Section III is devoted to an explanation of the large-N_c prediction, and the calculation of the form factors in chiral perturbation theory is performed in Sec. IV. In Sec. V we discuss the threshold form factors, whereas the phenomenology of K_{l4} and $\pi\pi$ scattering is considered in Sec. VI. After the algebraic part of the work described in this paper was finished, we received a paper by Bijnens[10] which also treats K_{l4} in chiral perturbation theory. We comment on the comparison of our work and his in this section also. Finally, we end with a summary and some comments on how future rare-kaon-decay experiments could help to test the chiral and large-N_c predictions more exactly.

II. FORM FACTORS AND EXPERIMENT IN K_{l4} DECAYS

We begin by defining the hadronic matrix element for the decay

$$K^+(k) \to \pi^+(p_+) + \pi^-(p_-) + e^+(p_e) + \nu(p_\nu) \ , \tag{1}$$

which may proceed through either the vector or axial-vector current. In the following we disregard all isospin-breaking effects. The vector-current matrix element has the form[4]

$$\langle \pi^+(p_+)\pi^-(p_-)\text{out}|V_\mu|K^+(k)\rangle = \frac{H}{m_K^3}\epsilon_{\mu\nu\alpha\beta}k^\nu(p_+ + p_-)^\alpha(p_+ - p_-)^\beta \tag{2}$$

while that of the axial vector is

$$\langle \pi^+(p_+)\pi^-(p_-)\text{out}|A_\mu|K^+(k)\rangle = \frac{-i}{m_K}[F(p_+ + p_-)_\mu + G(p_+ - p_-)_\mu + R(k - p_+ - p_-)_\mu] \ . \tag{3}$$

The four form factors F,G,R,H are functions of three variables, which may be chosen to be[2]

$$\begin{aligned} &s_\pi = (p_+ + p_-)^2 \ , \\ &s_l = (p_e + p_\nu)^2 = (k - p_+ - p_-)^2 \ , \\ &\theta_\pi \ , \end{aligned} \tag{4}$$

where θ_π is the angle in the $\pi\pi$ center of mass between the π^+ direction and a unit vector along the direction of recoil of the $\pi\pi$ system. Below we will also use the variables

$$t = (p_+ - k)^2, \quad u = (p_- - k)^2 \ , \tag{5}$$

which are related to s_π, s_l, and θ_π by

$$\begin{aligned} &t + u = 2m_\pi^2 + m_K^2 - s_\pi + s_l \ , \\ &t - u = -\left[1 - \frac{4m_\pi^2}{s_\pi}\right]^{1/2}[(m_K^2 - s_\pi - s_l)^2 - 4s_\pi s_l]^{1/2}\cos\theta_\pi \ . \end{aligned} \tag{6}$$

There may also be other K_{l4} decays: namely,

$$K^+ \to \pi^0\pi^0 e^+\nu, \quad K_L \to \pi^-\pi^0 e^+\nu \ . \tag{7}$$

These involve the same form factors as displayed in Eqs. (2) and (3). Let us denote by A^{-+}, A^{00}, and A^{-0} the current matrix elements of the processes (1) and (7). These are related by isospin symmetry:

$$A^{-+} = A^{00} + A^{-0} \ . \tag{8}$$

This relation also holds for the individual form factors. Each of the form factors may be decomposed into a piece which is symmetric or antisymmetric under $t \leftrightarrow u$. Because of Bose symmetry and of the $\Delta I = \frac{1}{2}$ nature of the current one has

$$\begin{aligned} &F_-^{00} = G_+^{00} = H_+^{00} = R_-^{00} = 0 \ , \\ &F_+^{-0} = G_-^{-0} = H_-^{-0} = R_+^{-0} = 0 \ , \end{aligned} \tag{9}$$

where F_-^{00} denotes the odd part of the form factor F^{00}. Together with the isospin relation Eq. (8) one finds that the nonvanishing parts in the form factors for the decays Eq. (7) are fixed by the form factors of $K^+ \to \pi^-\pi^+e^+\nu$:

$$I_\pm^{ij} = I_\pm^{-+}, \quad I = F,G,H,R \tag{10}$$

for all combinations aside from those detailed in Eq. (9).

The form factors may be written in a partial-wave expansion in the variable θ_π, such that the dependence on θ_π is transferred into a dependence on the relevant $\pi\pi$ partial-wave number. When the hadronic current is combined with the leptonic current to form the full matrix element, the effect of the R form factor becomes proportional to the electron mass, and hence unobservably small. We will not consider R further. The F form factor starts out with an S-wave contribution, while G and H have the P wave as the lowest nonvanishing partial wave: i.e.,

$$\begin{aligned} &F = f_S e^{i\delta_S} + f_p e^{i\delta_P}\cos\theta_\pi + D \text{ wave} \ , \\ &G = g e^{i\delta_P} + D \text{ wave}, \quad H = h e^{i\delta_P} + D \text{ wave} \ . \end{aligned} \tag{11}$$

Here δ_i is a strong final-state phase from scattering of the two pions. The form factors f_S, f_P, g, and h are real in the approximation considered here. [The expansion (11) is valid only if D-wave contributions in the final state are absent. The partial-wave expansion of the form factors in the general case is considerably more complicated.[2,3]]

Experimentally the study of K_{l4} decays is dominated by the work of Rosselet *et al.*,[11] which measures the $\pi^+\pi^-$ final state with good statistics. We therefore concentrate on $K^+ \to \pi^+\pi^-e^+\nu_e$ and compare directly with the results of Ref. 11.

Despite the good statistics, the experiment has not been able to separate out the full kinematic behavior of the matrix elements. Therefore certain approximations and/or assumptions have had to be made. For example, no dependence on s_l was seen within the limits of the data, so that results were quoted assuming that such dependence is absent. Similarly, f_P was found to be compatible with zero, and hence set equal to zero when the final result for g was derived. A dependence on s_π is seen, and is treated in the following manner. One defines reduced form factors $\bar{g} \equiv g/f_S$ and $\bar{h} \equiv h/f_S$ such that the decay rate has the form

$$d\Gamma = |f_S(s_\pi)|^2 d\bar{\Gamma}(\bar{g}(s_\pi), \bar{h}(s_\pi), \ldots) , \tag{12}$$

where the ellipses denote the kinematic variables $s_\pi, s_l, \ldots$. No linear dependence on s_π was seen within the errors for $\bar{g}$ and $\bar{h}$. Therefore $\bar{g}, \bar{h}$ were assumed to be constant, and all remaining s_π dependence was assumed to be in f_S, which was parametrized as

$$\begin{aligned} f_S(q^2) &= f_S(0)(1+\lambda_f q^2) , \\ q^2 &= (s_\pi - 4m_\pi^2)/4m_\pi^2 . \end{aligned} \tag{13}$$

Under the assumption of constant $\bar{g}, \bar{h}$, this means that g and h must share the same s_π behavior:

$$\begin{aligned} g(q^2) &= g(0)(1+\lambda_g q^2) , \\ h(q^2) &= h(0)(1+\lambda_h q^2) \end{aligned} \tag{14}$$

with the same λ, i.e., $\lambda_f = \lambda_g = \lambda_h = \lambda$. Finally all D-wave contributions were assumed to be absent.

These approximations to the form factors do not agree completely with what is found in the theoretical predictions. Dependence on s_l and nonzero values for f_P and D waves all occur in the theoretical results. In addition the s_π dependence is in general expected to be different in f_S, g, and h, although it can be forced to be identical if this is required. Such differences then cause some minor difficulty in comparing theory and experiment. In our fits we attempt to duplicate the experimental procedure as best we can in order to extract the low-energy constants that we are after, see Sec. VI.

The experimental results are then summarized by the following numbers:[11]

$$\begin{aligned} f_S(0) &= 5.59 \pm 0.14 , \\ g(0) &= 4.77 \pm 0.27 , \\ h(0) &= -2.68 \pm 0.68 , \\ \lambda &= 0.08 \pm 0.02 . \end{aligned} \tag{15}$$

We have used $|V_{us}| = 0.220$ in transcribing these results.

III. CHIRAL EXPANSION AND LARGE N_c

At low energies, QCD reduces to a theory of pions, kaons and η's interacting with each other and with the gauge bosons. These interactions are strongly constrained by the chiral symmetry of QCD.[5-7] All such interactions are described by an expansion in powers of the energy, and the lowest-order coefficients are uniquely predicted in terms of the pion decay constant, $F_\pi = 93.3$ MeV, and pion and kaon masses. At the next order in the energy expansion, there exist relations between processes parametrized by a small set of low-energy constants. This procedure, chiral perturbation theory, is best described in terms of nonlinear effective Lagrangians. At lowest order, called $O(E^2)$, the chiral Lagrangian is

$$\begin{aligned} \mathcal{L}_2 &= \frac{F^2}{4}\mathrm{Tr}(D_\mu U\, D^\mu U^\dagger) + \frac{F^2}{4}\mathrm{Tr}(\chi^\dagger U + \chi U^\dagger) , \\ D_\mu U &= \partial_\mu U - iR_\mu U + iUL_\mu , \\ U &= \exp(i\lambda^A \phi^A / F), \quad \chi = 2B_0 M , \end{aligned} \tag{16}$$

Here ϕ^A, $A = 1, \ldots, 8$, are the fields of the pseudoscalar octet, L_μ (R_μ) are the left-handed (right-handed) external gauge fields, $M = \mathrm{diag}(m_u, m_d, m_s)$ is the quark mass matrix and B_0 is a constant. In the remainder of this paper we work in the isospin limit $m_u = m_d$. At order E^2 we can then equate

$$\begin{aligned} & F_\pi = F, \quad m_\pi^2 = 2B_0 \hat{m} , \\ & m_K^2 = B_0(m_s + \hat{m}) , \\ & m_\eta^2 = \tfrac{4}{3}m_K^2 - \tfrac{1}{3}m_\pi^2, \quad \hat{m} = \tfrac{1}{2}(m_u + m_d) . \end{aligned} \tag{17}$$

Transition amplitudes are found (at this order) simply by expanding $\mathcal{L}_2$ in powers of the fields, and taking tree-level matrix elements.

At order E^4, the possible structure is somewhat more elaborate. Generalizing momentarily to N_f flavors, the chiral Lagrangian has the form[7]

$$\begin{aligned} \mathcal{L}_4 = {} & K_1[\mathrm{Tr}(D^\mu U^\dagger D_\mu U)]^2 + K_2 \mathrm{Tr}(D_\mu U^\dagger D_\nu U)\mathrm{Tr}(D^\mu U^\dagger D^\nu U) + K_3 \mathrm{Tr}(D^\mu U^\dagger D_\mu U\, D^\nu U^\dagger D_\nu U) \\ & + K_4 \mathrm{Tr}(D^\mu U^\dagger D^\nu U\, D_\mu U^\dagger D_\nu U) + L_4 \mathrm{Tr}(D^\mu U^\dagger D_\mu U)\mathrm{Tr}(\chi^\dagger U + \chi U^\dagger) + L_5 \mathrm{Tr}[D^\mu U^\dagger D_\mu U(\chi^\dagger U + U^\dagger \chi)] \\ & + L_6[\mathrm{Tr}(\chi^\dagger U + \chi U^\dagger)]^2 + L_7[\mathrm{Tr}(\chi^\dagger U - \chi U^\dagger)]^2 + L_8 \mathrm{Tr}(\chi^\dagger U \chi^\dagger U + \chi U^\dagger \chi U^\dagger) - iL_9 \mathrm{Tr}(R_{\mu\nu} D^\mu U\, D^\nu U^\dagger \\ & + L_{\mu\nu} D^\mu U^\dagger D^\nu U) + L_{10} \mathrm{Tr}(U^\dagger R_{\mu\nu} U L^{\mu\nu}) + H_1 \mathrm{Tr}(R_{\mu\nu} R^{\mu\nu} + L_{\mu\nu} L^{\mu\nu}) + H_2 \mathrm{Tr}(\chi^\dagger \chi) , \end{aligned} \tag{18}$$

where $L_{\mu\nu}$ and $R_{\mu\nu}$ are the field-strength tensors for L_μ, R_μ. In the case of three flavors one of the first four operators is redundant, and $\mathcal{L}_4$ starts out as

$$\begin{aligned} \mathcal{L}_4 = {} & L_1[\mathrm{Tr}(D^\mu U^\dagger D_\mu U)]^2 + L_2 \mathrm{Tr}(D_\mu U^\dagger D_\nu U)\mathrm{Tr}(D^\mu U^\dagger D^\nu U) + L_3 \mathrm{Tr}(D^\mu U^\dagger D_\mu U D^\nu U^\dagger D_\nu U) \\ & + L_4 \mathrm{Tr}(D^\mu U^\dagger D_\mu U)\mathrm{Tr}(\chi^\dagger U + \chi U^\dagger) + \cdots , \end{aligned} \tag{19}$$

where

$$L_1=K_1+\tfrac{1}{2}K_4,\quad L_2=K_2+K_4,\quad L_3=K_3-2K_4\ . \tag{20}$$

In the case of two flavors, two more low-energy constants may be eliminated as being redundant. Most important for our purposes is the fact that, among L_1,L_2,L_3, only the combinations L_2 and $(2L_1+L_3)$ enter into the $\pi\pi$ scattering amplitudes. At order E^4 one must include both loop diagrams, formed using $\mathcal{L}_2$, and tree diagrams from $\mathcal{L}_2$ and $\mathcal{L}_4$. In addition one includes the effect of the axial anomaly by using the Wess-Zumino-Witten anomaly Lagrangian.[12] The parameters $L_1,\ldots,L_{10}$ are in general divergent (except L_3,L_7). They absorb the divergences of the one-loop graphs. Consequently they will depend on a renormalization scale μ which, of course, drops out in all observable quantities. The renormalized parameters L_i^r are defined by

$$L_i=L_i^r+\frac{\Gamma_i}{16\pi^2}\mu^{d-4}\left[\frac{1}{d-4}-\frac{1}{2}[\ln(4\pi)+\Gamma'(1)+1]\right]$$

with Γ_i being pure numbers given in Ref. 7(a). The low-energy constants L_i^r cannot be determined from symmetry requirements alone—chiral symmetry only relates different processes, it does not provide the absolute normalization. However, most of the new coupling constants can be determined from low energy phenomenology.[5,7(a)] Furthermore, progress has been made in understanding their origin and their magnitude.[13,14] We are now able to estimate several of the coupling constants occurring at order E^4 on theoretical grounds, such that essentially parameter-free predictions can be made at this order of the chiral expansion.

The analysis of Ref. 7(a) makes use of the large-N_c suppression of the coupling constants $2L_1-L_2,L_4,L_6$, see below. Since the value of the coupling constants is of importance later in this article, we quote in Table I the values $L_i^r(\mu)$ at the scale $\mu=m_\eta$ according to that analysis.

The large-N_c limit enters in the following way. A trace in the chiral Lagrangian comes from a summation over the N_f flavors of quarks. Operators with two traces require at least two quark loops in order to get two summations over the flavors, while those with one trace require only a single quark loop. However, the large-N_c limit (with $\alpha_s N_c$ fixed) has the feature that processes with extra quark loops are suppressed by powers of $1/N_c$.[8,15] Therefore the coefficients of double trace operators, i.e., K_1,K_2,L_4,L_6, are suppressed by $1/N_c$ compared to the single trace coefficients $K_3,K_4,L_5,L_8,L_9,L_{10}$. ($L_7$ is an exception[7(a)] due to the η' pole contribution, as the η' mass vanishes in the large-N_c limit.) The single trace terms enter at order N_c so that the precise expectation is

$$\begin{aligned}&K_3,K_4,L_5,L_8,L_9,L_{10}=O(N_c)\ ,\\&K_1,K_2,L_4,L_6=O(1)\ .\end{aligned} \tag{21}$$

If one now specializes to the case of 3 flavors, one sees from Eq. (20) that the large-N_c limit requires

$$L_1,L_2,L_3=O(N_c),\quad L_2-2L_1=O(1)\ . \tag{22}$$

TABLE I. Values of the low-energy constants at the scale $\mu=m_\eta$ from Ref. 7(a). That analysis is based on the large-N_c suppression of $2L_1^r-L_2^r,L_4^r$ and L_6^r.

	$10^3L_i^r(m_\eta)$
L_1^r	0.9 ± 0.3
L_2^r	1.7 ± 0.7
L_3	-4.4 ± 2.5
L_4^r	0.0 ± 0.5
L_5^r	2.2 ± 0.5
L_6^r	0.0 ± 0.3
L_7	-0.4 ± 0.15
L_8^r	1.1 ± 0.3
L_9^r	7.4 ± 0.7
L_{10}^r	-6.0 ± 0.7

The ordering (21) and (22) has gone into the determination of the couplings L_i in Ref. 7(a). In particular, the value $L_3=(-4.4\pm2.5)\times10^{-3}$ used in the evaluation of $\eta\to3\pi$ to one loop in Ref. 7(c) is based on the large-N_c suppression of L_2-2L_1. K_{l4} decays make it possible to test the ordering (22) which cannot be probed using only pions.

IV. CHIRAL PREDICTIONS FOR THE FORM FACTORS

The chiral representation of the form factors at order E^2 was originally given by Weinberg:[9]

$$F=G=\frac{m_K}{\sqrt{2}F_\pi}=3.74,\quad H=0\ . \tag{23}$$

(Unless stated otherwise, we use in all numerical calculations $m_K=m_{K^+}=493.7$ MeV, $m_\pi=m_{\pi^+}=139.6$ MeV, $F_\pi=93.3$ MeV.) At order E^4, loops with $\mathcal{L}_2$ and tree-level contributions from $\mathcal{L}_4$ both enter. We have used the general one-loop Lagrangian given in Eqs. (8.12) and (8.13) of Ref. 7(a) for the evaluation of F and G. We write the result for F in the form

$$\begin{aligned}F(s_\pi,t,u)&=\frac{m_K}{\sqrt{2}F_\pi}[1+F^+(s_\pi,t,u)+F^-(s_\pi,t,u)\\&\qquad+O(E^4)]\ ,\\F^\pm(s_\pi,t,u)&=U_F^\pm(s_\pi,t,u)+P_F^\pm(s_\pi,t,u)+C_F^\pm\end{aligned} \tag{24}$$

and will use below an analogous expression for the form factor G. The superscript $+$ $(-)$ denotes a term which is even (odd) under crossing $t\leftrightarrow u$. The contributions $U_F^\pm(s_\pi,t,u)$ denote the unitary corrections generated by the one-loop graphs which appear at order E^4. They have the form

$$\begin{aligned}U_F^+(s_\pi,t,u)&=F_\pi^{-2}[\Delta_0(s_\pi)+a_F(t)+a_F(u)]\ ,\\U_F^-(s_\pi,t,u)&=F_\pi^{-2}[b_F(t)-b_F(u)]\end{aligned} \tag{25}$$

with

$$
\begin{aligned}
\Delta_0(s_\pi)&=\tfrac{1}{2}(2s_\pi-m_\pi^2)J^r_{\pi\pi}(s_\pi)+\frac{3s_\pi}{4}J^r_{KK}(s_\pi)+\frac{m_\pi^2}{2}J^r_{\eta\eta}(s_\pi)\\
a_F(t)&=\tfrac{1}{32}[(14m_K^2+14m_\pi^2-19t)J^r_{K\pi}(t)+(2m_K^2+2m_\pi^2-3t)J^r_{\eta K}(t)]\\
&\quad+\tfrac{1}{16}[(3m_K^2-7m_\pi^2+5t)K_{K\pi}(t)+(m_K^2-5m_\pi^2+3t)K_{\eta K}(t)]\\
&\quad-\tfrac{1}{8}\{9[L_{K\pi}(t)+L_{\eta K}(t)]+(3m_K^2-3m_\pi^2-9t)[M^r_{K\pi}(t)+M^r_{\eta K}(t)]\}\ ,\\
b_F(t)&=a_F(t)-\tfrac{1}{2}(m_K^2+m_\pi^2-t)J^r_{K\pi}(t)\ .
\end{aligned}
\tag{26}
$$

The loop integrals $J^r_{\pi\pi}(s_\pi),\ldots$ which occur in these expressions are listed in the Appendix. The functions J^r_{PQ} and M^r_{PQ} depend on the scale μ at which the loops are renormalized. The scale drops out in the expression for the full amplitude, see below. The imaginary part of $F_\pi^{-2}\Delta_0(s_\pi)$ contains the $I=0$, S-wave $\pi\pi$ phase shift

$$\delta_0^0(s_\pi)=(32\pi F_\pi^2)^{-1}(2s_\pi-m_\pi^2)\left[1-\frac{4m_\pi^2}{s_\pi}\right]^{1/2}+O(E^4) \tag{27}$$

as well as contributions from $K\bar{K}$ and $\eta\eta$ intermediate states. The functions $a_F(t)$ and $b_F(t)$ are real in the physical region.

The contribution $P_F^{\pm}(s_\pi,t,u)$ is a polynomial in s_π,t,u, obtained from the tree graphs at order E^4. We find

$$P_F^{\pm}(s_\pi,t,u)=\frac{1}{F_\pi^2}\sum_{i=1}^{9}P^{\pm}_{i,F}(s_\pi,t,u)L_i^r\ , \tag{28}$$

where

$$
\begin{aligned}
P^+_{1,F}&=32(s_\pi-2m_\pi^2)\ ,\\
P^+_{2,F}&=8(2m_K^2+2m_\pi^2-t-u)\\
&=8(m_K^2+s_\pi-s_l)\ ,\\
P^+_{3,F}&=2(2m_K^2-6m_\pi^2+4s_\pi-t-u)\\
&=2(m_K^2-8m_\pi^2+5s_\pi-s_l)\ ,\\
P^+_{4,F}&=32m_\pi^2,\quad P^+_{5,F}=4m_\pi^2\ ,\\
P^+_{9,F}&=2(-m_K^2-2m_\pi^2+s_\pi+t+u)=2s_l\ ,\\
P^-_{3,F}&=-2(t-u)\\
&=2\left[1-\frac{4m_\pi^2}{s_\pi}\right]^{1/2}[(m_K^2-s_\pi-s_l)^2-4s_\pi s_l]^{1/2}\cos\theta_\pi\ .
\end{aligned}
\tag{29}
$$

The remaining coefficients $P^{\pm}_{i,F}$ are zero. The symbols L_i^r denote the renormalized coupling constants discussed above.

Finally we come to the contributions $C_F^{\pm}$ which contain logarithmic terms, independent of s_π, t, and u:

$$
\begin{aligned}
C_F^+&=(256\pi^2F_\pi^2)^{-1}\\
&\quad\times\left[5m_\pi^2\ln\frac{m_\pi^2}{\mu^2}-2m_K^2\ln\frac{m_K^2}{\mu^2}-3m_\eta^2\ln\frac{m_\eta^2}{\mu^2}\right]\ ,\\
C_F^-&=0\ .
\end{aligned}
\tag{30}
$$

The corresponding decomposition of the form factor G,

$$G^{\pm}=U_G^{\pm}+P_G^{\pm}+C_G^{\pm}\ , \tag{31}$$

has the explicit form

$$
\begin{aligned}
U_G^+(s_\pi,t,u)&=F_\pi^{-2}[\Delta_1(s_\pi)+a_G(t)+a_G(u)]\ ,\\
U_G^-(s_\pi,t,u)&=F_\pi^{-2}[b_G(t)-b_G(u)]
\end{aligned}
\tag{32}
$$

with

$$
\begin{aligned}
\Delta_1(s_\pi)&=2s_\pi[M^r_{\pi\pi}(s_\pi)+\tfrac{1}{2}M^r_{KK}(s_\pi)]\ ,\\
a_G(t)&=\tfrac{1}{32}[(2m_K^2+2m_\pi^2+3t)J^r_{K\pi}(t)-(2m_K^2+2m_\pi^2-3t)J^r_{\eta K}(t)]\\
&\quad+\tfrac{1}{16}[(-3m_K^2+7m_\pi^2-5t)K_{K\pi}(t)+(-m_K^2+5m_\pi^2-3t)K_{\eta K}(t)]\\
&\quad-\tfrac{3}{8}\{L_{K\pi}(t)+L_{\eta K}(t)-(m_K^2-m_\pi^2+t)[M^r_{K\pi}(t)+M^r_{\eta K}(t)]\}\ ,\\
b_G(t)&=a_G(t)-\tfrac{1}{2}(m_K^2+m_\pi^2-t)J^r_{K\pi}(t)\ .
\end{aligned}
\tag{33}
$$

The imaginary part of $F_\pi^{-2}\Delta_1(s_\pi)$ contains the $I=1$, P-wave phase shift

$$\delta_1^1(s_\pi)=(96\pi F_\pi^2)^{-1}(s_\pi-4m_\pi^2)\left[1-\frac{4m_\pi^2}{s_\pi}\right]^{1/2}+O(E^4) \tag{34}$$

as well as contributions from $K\bar{K}$ intermediate states. The functions a_G,b_G are real in the physical region.

The polynomials

$$P_G^{\pm}=\frac{1}{F_\pi^2}\sum_{i=1}^{9}P^{\pm}_{i,G}(s_\pi,t,u)L_i^r \tag{35}$$

TABLE II. Determination of the low-energy constants from various sets of data. The column labeled TEB indicates the possible inclusion of theoretical error bars applied to the analysis as described in the text. The running scale is taken at $\mu=m_\eta$. Error bars correspond to an increase of χ^2 by 1.

Comments	TEB	$10^3L_1^r$	$10^3L_2^r$	10^3L_3
(a) $f_S(0),g(0),\lambda_f$	No	0.69 ± 0.30	1.99 ± 0.32	-3.21 ± 1.05
(b) $f_S(0),g(0),\lambda_f$	Yes	0.69 ± 0.54	1.99 ± 1.15	-3.21 ± 1.50
(c) $n(s_\pi),\bar{g}(s_\pi),f_S(0)$	No	0.70 ± 0.23	2.04 ± 0.34	-3.35 ± 0.92
(d) $n(s_\pi),\bar{g}(s_\pi),f_S(0)$	Yes	0.66 ± 0.74	2.04 ± 1.81	-3.27 ± 3.49
(e) $f_S(0),g(0),\lambda_f,\delta_0^0-\delta_1^1$	No	0.68 ± 0.30	1.97 ± 0.32	-3.13 ± 1.06
(f) $f_S(0),g(0),\lambda_f,\delta_0^0-\delta_1^1$	Yes	0.57 ± 0.53	2.38 ± 1.10	-3.08 ± 1.50
(g) $f_S(0),g(0),\lambda_f$, scattering lengths	No	0.66 ± 0.30	1.90 ± 0.26	-3.13 ± 0.94
(h) $f_S(0),g(0),\lambda_f$, scattering lengths	Yes	0.91 ± 0.47	1.62 ± 0.37	-3.76 ± 1.31

are

$$
\begin{aligned}
P_{3,G}^{+}&=-2(2m_K^2+2m_\pi^2-t-u)\\
&=-2(m_K^2+s_\pi-s_l)\ ,\\
P_{5,G}^{+}&=4m_\pi^2\ ,\\
P_{9,G}^{+}&=2(-m_K^2-2m_\pi^2+s_\pi+t+u)=2s_l\ ,\\
P_{2,G}^{-}&=8(t-u)\\
&=-8\left[1-\frac{4m_\pi^2}{s_\pi}\right]^{1/2}\\
&\qquad\times[(m_K^2-s_\pi-s_l)^2-4s_\pi s_l]^{1/2}\cos\theta_\pi\ ,\\
P_{3,G}^{-}&=\tfrac{1}{4}P_{2,G}^{-}\ .
\end{aligned}
\tag{36}
$$

The remaining $P_{i,G}^{\pm}$ vanish. The logarithms contained in $C_G^{\pm}$ are

$$C_G^{\pm}=-C_F^{\pm}\ . \tag{37}$$

The form factor H starts only at $O(E^4)$. It does not appear in the Lagrangian of Eqs. (18) and (19), but arises from the Wess-Zumino-Witten Lagrangian for the axial anomaly.[12] It is related by an SU(3) transformation to the anomalous $\gamma\to3\pi$ coupling. The prediction is

$$H=\frac{\sqrt{2}m_K^2}{8\pi^2F_\pi^3}=2.65 \tag{38}$$

in excellent agreement with the experimental value. To the order we are working, we do not consider loops or higher-order corrections to this result. The form factor H gives rise to an interference term $\sim GH^*+G^*H$ in the decay distribution $d\Gamma$. We have checked that the sign of this term, evaluated according to our phase convention for H and G, agrees with the one given by Rosselet *et al.* (Ref. 11, Table II).

The results for F and G must satisfy two nontrivial constraints: (i) Unitarity requires that F and G contain, in the physical region $4m_\pi^2\le s_\pi\le m_K^2$, imaginary parts governed by S- and P-wave $\pi\pi$ scattering [these imaginary parts are contained in the functions $\Delta_0(s_\pi),\Delta_1(s_\pi)$]; (ii) the scale dependence of the low-energy constants L_i^r must be compensated for by the scale dependence of $U_{F,G}$ and $C_{F,G}$ for all values of s_π,t,u,m_π^2,m_K^2. (Since we work at order E^4, the meson masses appearing in the above expressions satisfy the Gell-Mann–Okubo mass formula.) We have checked that these constraints are satisfied. Furthermore, our expressions agree algebraically with the ones given by Bijnens.[10] (In order to compare with the latter, the pion decay constant F_π must also be expanded around the chiral limit $m_u=m_d=m_s=0$.)

V. EXPANSION OF FORM FACTORS AT THRESHOLD

In the chiral predictions of the form factors, one striking feature that emerges from Eqs. (29) and (36) is that the only important dependence on the low-energy constants is through L_1, L_2, and L_3. Furthermore, L_1 and L_2 are absent in the isospin even part G^+. The influence of L_4,L_5 is proportional to m_π^2 and hence is too small to be of much importance. This means that we are not able to test the large-N_c prediction that $L_4/L_1\simeq0$. In addition, the constant L_9 enters only in the s_l dependence, which again is not large and which has been dropped from the experimental analysis. We proceed by fixing L_4, L_5, and L_9 at the values found in other processes, as quoted in Ref. 7(a) [i.e., $L_4=0$ from the Zweig rule, L_5 from F_K/F_π and L_9 from the electromagnetic charge radius of the pion, see also Table I].

Before describing the detailed comparison with the data, we discuss the form factors at threshold, because the results can be presented simply at this kinematical point. We define the projected amplitudes

$$
\begin{aligned}
f(q^2,s_l)&=\tfrac{1}{2}\int_{-1}^{1}d(\cos\theta_\pi)\mathrm{Re}F(q^2,s_l,\cos\theta_\pi)\ ,\\
q^2&=\frac{s_\pi-4m_\pi^2}{4m_\pi^2}
\end{aligned}
\tag{39}
$$

and similarly for $g(q^2,s_l)$. Taking the real part $\mathrm{Re}F$ eliminates the phase at this order in the low-energy expansion. We renormalize all of the low-energy constants at the scale $\mu=m_\eta$ and write the form factors as

$$
\begin{aligned}
f(q^2,s_l)&=f(0,s_l)[1+\lambda_f(s_l)q^2+O(q^4)]\ ,\\
g(q^2,s_l)&=g(0,s_l)[1+\lambda_g(s_l)q^2+O(q^4)]\ .
\end{aligned}
\tag{40}
$$

First we consider the threshold form factors

$$f(0,0)=\frac{m_K}{\sqrt{2}F_\pi}\left[1+X_f+\frac{2}{F_\pi^2}[32m_\pi^2L_1^r+4(m_K^2+4m_\pi^2)L_2^r+(m_K^2+12m_\pi^2)L_3+16m_\pi^2L_4^r+2m_\pi^2L_5^r]+O(E^4)\right],$$
$$g(0,0)=\frac{m_K}{\sqrt{2}F_\pi}\left[1+X_g-\frac{2}{F_\pi^2}[(m_K^2+4m_\pi^2)L_3-2m_\pi^2L_5^r]+O(E^4)\right]. \tag{41}$$

The constants X_f, X_g contain loop and tadpole contributions:

$$\begin{array}{lllll} X_f & =0.185 & -0.051 & -0.007 & =0.127, \\ X_g & =0.023 & -0.030 & +0.007 & =0, \\ & \pi\pi & K\bar{K},\eta\eta & \text{tadpoles} & \\ & \text{loops} & K\pi,K\eta & & \\ & & \text{loops} & & \end{array} \tag{42}$$

where the pieces denoted by "tadpoles" come from the logarithms collected in C_F^+, C_G^+ defined in Eqs. (30) and (37). It is seen that the major portion of the one-loop correction X_f is due to $\pi\pi$ final-state interactions. As emphasized in particular by Truong,[16] this is a rule rather than an exception: Pions in $I=0$, S-wave final states tend to produce potentially large corrections to the lowest-order term in many hadronic processes.

Inserting into Eq. (41) the values for L_i^r from Table I one finds $f(0,0)=4.85$, $g(0,0)=5.03$. The increase from the tree result $f_{\text{tree}}=g_{\text{tree}}=3.74$ to $g(0,0)=5.03$ is dominantly due to the effect of L_3, as the loops do not contribute to the amplitude $g(0,0)$ according to Eq. (42) and the dependence on L_5 is weak due to the factor of m_π^2. (Pions in the $I=1$, P wave interact weakly. An analogous result holds for the $I=1$, P wave in elastic $\pi\pi$ scattering.[13]) At $s_l=s_l^{\max}=(m_K-2m_\pi)^2$, the results change little: $X_f\to 0.129$, $f(0,0)\to 5.05$, and $X_g\to -0.003, g(0,0)\to 5.14$. Now we consider the slopes λ_f, λ_g. we find

$$\lambda_f(s_l)=Y_f(s_l)+\frac{8m_\pi^2}{F_\pi^2}(16L_1^r+4L_2^r+5L_3)+O(E^4),$$
$$\lambda_g(s_l)=Y_g(s_l)-\frac{8m_\pi^2}{F_\pi^2}L_3+O(E^4), \tag{43}$$

where Y_f, Y_g contain loop contributions:

$$Y_f(s_l) \quad =0.11 \quad -0.034 \quad (-0.029) \quad =0.076 \quad (0.081), \tag{44}$$

$$\begin{array}{llllll} Y_g(s_l) & =0.042 & +0.003 & (+0.001) & =0.045 & (0.043), \\ & \pi\pi & K\bar{K},\eta\eta & & & \\ & \text{loops} & K\pi,K\eta & & & \\ & & \text{loops} & & & \end{array}$$

The numbers in parentheses denote the values at $s_l=s_l^{\max}$. Again the largest contribution arises from $\pi\pi$ interactions. The values of L_1, L_2, and L_3 from Table I give

$$\lambda_f=0.06\ (0.07),\quad \lambda_g=0.12\ (0.12). \tag{45}$$

Note that the loop effects almost saturate the experimental value for λ_f at $\mu=m_\eta$. This leaves little room for further contributions due to the low-energy constants L_i. This combination of constants must then not be very large, and in practice λ_f is a strong phenomenological constraint on L_i. As can be seen from Eq. (45), the values from Table I satisfy this constraint already.

VI. COMPARISON WITH EXPERIMENT

We will see that chiral perturbation theory can easily account for the K_{l4} data. In order to make this statement more precise, there are several ways that we can approach the data. At the simplest level, we can fit the extracted values of the threshold form factors and slopes $f_s(0)$, $g(0)$, and λ_f. In the data, a dependence on s_l was not seen, although of course there is a small dependence. We take this into account by squaring the amplitude, averaging over s_l, then taking the square root:

$$f_S(s_\pi)=\left[\frac{1}{s_l^{\max}}\int_0^{s_l^{\max}}ds_l\left|\frac{1}{2}\int_{-1}^{1}d(\cos\theta_\pi)F(s_\pi,s_l,\cos\theta_\pi)\right|^2\right]^{1/2},$$
$$\lambda_f=\frac{1}{f_S(0)}\frac{d}{dq^2}f_S(q^2)\Bigg|_{q^2=0} \tag{46}$$

and similarly for g,λ_g. [In this article, $f_S(0)$, $g(0)$, and $h(0)$ always denote the form factors evaluated at $q^2=0$, see Eqs. (13) and (14).] This most nearly approximates the experimental situation. [Recall that the experimental analysis assumed that the slopes of $f_S(s_\pi)$ and $g(s_\pi)$ were the same, i.e., $\lambda_f=\lambda_g$. We will not include λ_g in our fitting procedure, but will treat it as a prediction, testing the level of equality of λ_f and λ_g.] However since the experimental form-factor analysis did not conform exactly to the structure of the chiral predictions, we can also attempt to compare our results more directly with the experimental data. The primary data consists of the numbers of events grouped into bins of energy, $n(s_\pi)$, plus the absolute normalization which is basically $f_S(0)$ and the P/S-wave ratio $\bar{g}(s_\pi)$. We can form these quantities from theory and compare to the experimental results for these variables. Our two options then are to use the sets $\{f_S(0), g(0), \lambda_f\}$ or $\{n(s_\pi), f_S(0), \bar{g}(s_\pi)\}$ for comparison. Given a perfect analysis, the two approaches should of course be the same, and the use of the two addresses the question of the compatibility of the chiral and experimental analysis. Fortunately we will see that very similar results emerge from both options.

A second issue is the question of the way to quantify the theoretical uncertainties in the analysis. Chiral perturbation theory is unique in the low-energy region, being a technique which is a controlled expansion. As such, it contains in its framework ways to estimate the uncertainties from the next order in the expansion. In this paper we are computing effects at order E^2 and order E^4, so that corrections arise from order E^6 and yet higher orders. Such corrections could influence the determination of the L_i coefficients. For example, if the data had infinite precision a naive fit to L_1, L_2, L_3 would yield values with infinitesimal error bars. However, this would not be a true estimate of the uncertainty in L_i, as corrections to the theoretical analysis from order E^6 could shift the values by more than an infinitesimal amount. We attempt to quantify this effect by including theoretical error bars in our fits. These are not required in order to obtain a good description, but are a fair estimate of the nature of the energy expansion. In those analyses labeled as containing theoretical error bars, they have been included in the following manner. Observables are generally of the form $a_{\text{expt}} = a_2(1 + c_4 + c_6 + \cdots)$ where a_2 is the lowest-order result (i.e., order E^2) and c_4 is a correction which we are computing at order E^4. We will use c_4 to estimate the next-order correction c_6, using the expectation that $c_6 = O(c_4^2) = O([(a_{\text{expt}} - a_2)/a_2]^2)$. Thus the theoretical prediction would be of the form

$$\begin{aligned} a_{\text{expt}} &= a_2(1 + c_4 \pm c_4^2) \\ &= a_2\left[1 + c_4 \pm \left[\frac{a_{\text{expt}} - a_2}{a_2}\right]^2\right] . \end{aligned} \tag{47}$$

It is the latter form which is used in our fitting procedure where it is added in quadrature to the experimental error. Our experience has been that the expansion in energy is uniform and that this is a fair assessment of the next-order term. The slope is a loop effect and there is thus no order E^2 correction to λ_f, λ_g in our analysis. We have assigned an error $\Delta\lambda_f$ which is 40% of its experimental value. [We have also checked in a few cases that the following procedure results in very similar error bars for L_1, L_2, and L_3. First we determined ΔL_i^e by assigning no theoretical error. Then we did a least-squares fit by changing the theoretical predictions by $(a_{\text{expt}} - a_2)^2/a_2$ in turn and then reading off the variation ΔL_i^t; finally we added ΔL_i^e and ΔL_i^t in quadrature.]

There is a last point which concerns the total decay rate Γ_{tot}. Below we show that the coupling constants L_1, L_2, and L_3 can be chosen such that the averaged form factors defined in Eq. (46) practically coincide with the measured ones. Nevertheless the total decay rate calculated with these form factors is $\sim 10\%$ below the measured value, which seems to indicate that the smearing over $s_l, \cos\theta_\pi$ described above does not correspond to the experimental analysis. We have noted, however, that the published experimental values[11] of $f_s(q^2), g(q^2)$ also produce too small a value for the decay rate: $\Gamma_{\text{tot}} = 2.94 \times 10^3\ \text{sec}^{-1}$ instead of $\Gamma_{\text{expt}} = 3.26 \times 10^3\ \text{sec}^{-1}$. (Note that the experimental value Γ_{expt} was used to normalize the form factors.) We do not understand this discrepancy.

The results of our procedures to fix L_1, L_2, and L_3 are displayed in Table II and Fig. 2. The first four rows in the table list the determination of the low-energy constants L_1, L_2, L_3 which follows from K_{l4} data alone. The error bars correspond to an increase in χ^2 by one. We see that there is good agreement with the central values in all cases. This indicates that the manner in which the

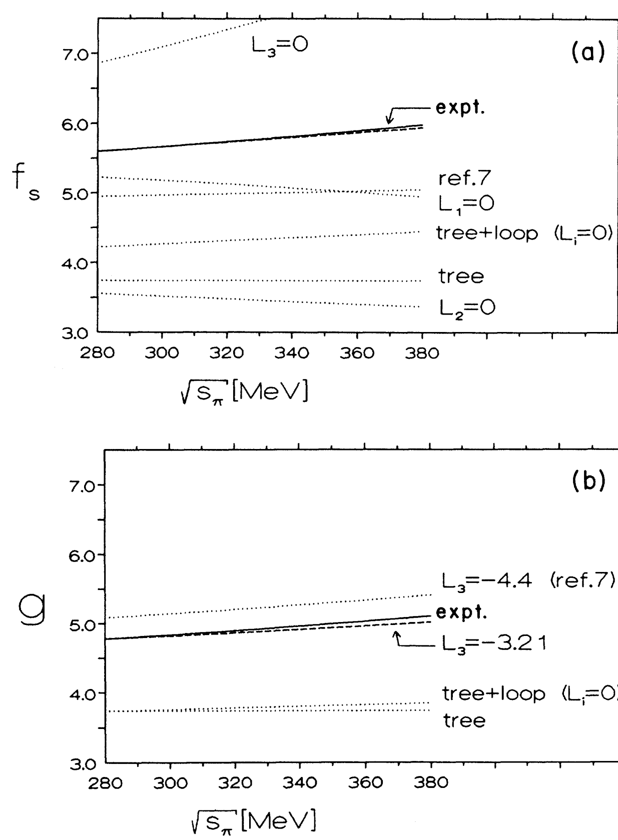

FIG. 2. The form factors $f_S(s_\pi)$ and $g(s_\pi)$ according to the chiral representation described in Sec. IV. Displayed are the lowest-order result (labeled "tree") plus the experimental and central values of fit (a) in Table II (solid and dashed line, respectively). We also show the effect of the loop terms by themselves as well as the effect of turning off each of the couplings L_1, L_2, L_3 in turn. Note that $g(s_\pi)$ does depend neither on L_1 nor on L_2.

analysis is done makes little difference, and that the theoretical error bars are not needed.

The figures give a better view of the results. On them are displayed the lowest-order result (labeled "tree") plus the experimental central value and the central values of fit (a) in Table II. In order to see the decomposition of the ingredients of the final results, we also show the effect of the loop terms by themselves as well as the effect of turning off each of the couplings $L_{1,2,3}$ in turn. Note that the slope of the g form factor has not been included in the fit and thus is a prediction. It matches very well with the experimental constraint that g/f_S is a constant.

We already mentioned that the P-wave part f_P was searched for but not found. We have evaluated f_P from the chiral representation (24) with the parameters corresponding to Table II(a). In particular, we have set $s_l=0$, $F(s_\pi,\cos\theta_\pi)=F_S+F_P\cos\theta_\pi+\cdots$. The P-wave term F_P indeed is very small, $|F_P|<5\times10^{-2}|F_S|$ over the whole energy range $4m_\pi^2<s_\pi<m_K^2$.

As we have indicated, one motivation for our analysis was to test the large-N_c prediction $(L_2-2L_1)/L_3=0$. From the values presented in Table II, we see that a small nonzero value for this ratio is preferred, but that it is consistent with zero within the errors. To make the error analysis cleaner, we have repeated the fitting procedures using the variables

$$\begin{aligned} &X_1=L_2-2L_1-L_3,\quad X_2=L_2\ ,\\ &X_3=(L_2-2L_1)/L_3\ . \end{aligned} \tag{48}$$

The first variable was chosen because in the SU(2) limit it measures the effect of the ρ in the $I=1$, $J=1$ $\pi\pi$ scattering. The last is clearly the large-N_c-violating combination. The resulting values [using $f_S(0),g(0),\lambda_f$] are

$$\begin{aligned} &X_1=(3.82\pm0.89)\times10^{-3}\ ,\\ &X_2=(1.99\pm0.32)\times10^{-3}\ ,\\ &X_3=-0.19^{+0.16}_{-0.27} \end{aligned} \tag{49}$$

without theoretical error bars and

$$\begin{aligned} &X_1=(3.82\pm2.10)\times10^{-3}\ ,\\ &X_2=(1.99\pm1.15)\times10^{-3}\ ,\\ &X_3=-0.19^{+0.55}_{-0.80} \end{aligned} \tag{50}$$

with them. The result is that the large-N_c prediction works remarkably well, at the level expected, within the error bars.

Having determined the low-energy constants, we are in a position to study the predictions of chiral symmetry. These same coefficients govern $\pi\pi$ scattering, and the real test of the theory is that they are simultaneously compatible with the $\pi\pi$ amplitudes.[5] The most straightforward way to check this is to predict the $\pi\pi$ scattering lengths. While the direct data at low energy is poor, the scattering lengths[17] have been obtained using the Roy equations to constrain both the high-and low-energy data.[18] The chiral predictions were worked out in Ref. 5. If we use our determination (a) in Table II, we obtain the predictions of Table III, third column. For $\bar{l}_3,\bar{l}_4$ which occur in a_l^I,b_l^I we have used the central values $\bar{l}_3=2.9,\bar{l}_4=4.3$ from Ref. 5. We do not quote errors in the threshold parameters evaluated here, because we did not work out the error matrix associated with the L_i's. The predictions are within $1\frac{1}{2}$ standard deviations of the measured values in all cases. We have also checked that the same parameters reproduce the full amplitudes within experimental and theoretical uncertainties up to $\sqrt{s_\pi}\approx m_K$.

Instead of treating the $\pi\pi$ data as predictions, one could use them in a different manner to influence the determination of the L_i's. The motivation for doing this is twofold: (i) it checks the consistency of the theory and (ii) it provides the best determination of the low-energy constants. Again, there are a few ways that we could proceed. The Rosselet K_{l4} experiment itself provides the only significant direct measurement of $\delta_0^0-\delta_1^1$ at low energies. We can include this in our analysis as well. The result is the coefficients of (e) and (f) of Table II. [We did not use theoretical errors in $\delta_0^0-\delta_1^1$, because we expect their effect, which is $O(m_\pi^4)$, to be small in the energy range considered here, $\sqrt{s_\pi}\leq380$ MeV.] One sees that

TABLE III. Predictions of chiral symmetry following from the fit to the K_{l4} data alone (column 3) and the combined determination from $\pi\pi$ and K_{l4} data (last column). The first column gives the prediction of the leading-order term in the low-energy expansion of the $\pi\pi$ amplitude.

	Leading order	Experiment (Ref. 17)	K_{l4} alone	$K_{l4}+\pi\pi$
λ_g		0.08 ± 0.02	0.06 ± 0.02	0.06 ± 0.02
a_0^0	0.16	0.26 ± 0.05	0.20	0.20
b_0^0	0.18	0.25 ± 0.03	0.26	0.26
a_0^2	-0.045	-0.028 ± 0.012	-0.040	-0.041
b_0^2	-0.089	-0.082 ± 0.008	-0.069	-0.070
a_1^1	0.030	0.038 ± 0.002	0.037	0.036
b_1^1			0.0045	0.0043
a_2^0		$(17\pm3)\times10^{-4}$	21×10^{-4}	20×10^{-4}
a_2^2		$(1.3\pm3)\times10^{-4}$	3.5×10^{-4}	3.5×10^{-4}

the same parameters describe the phase shift information, with a good fit $\chi^2/N_{DF}=0.82$ and 0.78. Instead of these direct data, one may compare with the experimental scattering lengths given in the second column of Table III. The result is displayed in (g) and (h) of Table II. [Here the $\chi^2/N_{DF}=1.0$ and 0.8. We did not associate theoretical errors with the threshold parameters, because these effects are $O(m_\pi^4)$ and thus very small.] The agreement of the chiral predictions described above is manifest in the fact that the central values do not change much between cases (a), (b) and (g), (h). We conclude that the theory is quite consistent with all sets of data.

The results of this analysis determine the value of the coefficients in the purely SU(2) chiral Lagrangian. In the notation of Ref. 5, the results of fit (g), (h) are

$$\bar{l}_1=-0.70\pm0.94\ (-0.97\pm1.22)\ ,$$
$$\bar{l}_2=6.31\pm0.49\ (5.77\pm0.72) \tag{51}$$

without (with) theoretical error bars. The central value of these can be easily obtained from linear combinations of L_1,L_2,L_3. To obtain the quoted error bars we have performed the fits using $L_3,\bar{l}_1,\bar{l}_2$ as the independent variables. The magnitude of the constant $\bar{l}_1$ is smaller than the estimate from the $\pi\pi$ analysis of Ref. 13, while that of $\bar{l}_2$ is essentially identical. Within the $\pi\pi$ system, the difference between the two determinations comes from differing treatment of the data at higher energies and is within the uncertainty of the $\pi\pi$ data and of the energy expansion. However, the study of the K_{l4} form factors adds strong additional constraints and the coefficient sets of this paper are to be preferred.

Finally, it is of interest to provide the best determination of the low-energy constants by including the maximum amount of data. This, of course, includes the K_{l4} form factors $f_S(0)$, $g(0)$, and λ, as well as the direct measurement of $\delta_0^0-\delta_1^1$ in K_{l4} decay. We take the other $\pi\pi$ information as the scattering lengths a_1^1,a_2^0,a_2^2,b_0^2 as well as the universal curve[17,19]

$$X(a_0^0,a_0^2)=2a_0^0-5a_0^2-0.96(a_0^0-0.3)-0.7(a_0^0-0.3)^2$$
$$=0.69\pm0.04\ . \tag{52}$$

This is a well-determined combination which is independent of the K_{l4} phase shift information. The results are shown in the first two rows of Table IV, with the resulting scattering lengths and slope λ_g given in Table III (last column). The χ^2/N_{DF} is 0.9, the error bars again correspond to an increase in χ^2 by one. For comparison we display in the fourth row the values of L_1, L_2, and L_3 determined in Refs. 5 and 7(a) from the D-wave $\pi\pi$ scattering lengths and the large-N_c suppression of $2L_1-L_2$. (Here the error bars have a different origin and meaning, see Refs. 5 and 7(a).)

The K_{l4} data on $\pi\pi$ scattering is not yet precise enough to address the question of alternate pictures of chiral-symmetry breaking, which seem to prefer a value of $a_0^0\simeq0.26$ instead of the usual value of $a_0^0=0.20\pm0.01$. (The literature on the subject may be traced from Ref. 20.) The data of Rosselet *et al.*[11] lead to $a_0^0=0.26\pm0.05$,[18,19] which is compatible with both values.

The nice agreement between the values for L_1, L_2, and L_3 found with these different approaches has implications on $\eta\to3\pi$ decays. Some time ago this process was evaluated to next-to-leading order in chiral perturbation theory.[7(c)] With the exception of L_3, all low-energy coupling constants which occur in the final expression for the matrix element can be absorbed into physical quantities. In Ref. 7(c) the value $L_3=-4.4\times10^{-3}$, determined as mentioned above from $\pi\pi$ D waves and large-N_c arguments, was used to evaluate the decay rate of $\eta\to3\pi$. The fact that K_{l4} data confirm this value according to Table IV means that the notorious difficulty to explain $\eta\to3\pi$ in chiral perturbation theory[7(c),21,22] cannot be blamed on an incorrect value of L_3 used in that calculation.

In Fig. 3 (curve 1), we show the form factors $f_S(s_\pi)$ and $g(s_\pi)$ corresponding to the values in the first row of Table IV. Numerically, these correspond to $f_S(0)=5.53$, $g(0)=4.74$, and $\lambda_f=0.08$, as well as the values quoted in the last column of Table III. The agreement with the data is excellent. To visualize the working of the large-N_c rule, we display also the form factors which result from the same fit, however with the additional constraint $L_2=2L_1$ (curve 2). Numerically, $2L_1=L_2=1.90$, $L_3=-3.74$, $\chi^2/N_{DF}=0.95$ or, equivalently $\bar{l}_1=-0.78,\bar{l}_2=6.3$. In Fig. 4 we also display the phase difference $\delta_0^0-\delta_1^1$ corresponding to the values in the first row of Table IV, together with the data from Ref. 11. The theoretical curve agrees with the measurements within the error bars, although the data appear to be systematically on the higher side. Note that the values of L_1, L_2, and L_3 used here lead to $a_0^0=0.20$ (see the last

TABLE IV. Determination of the chiral low-energy constants from the full set of low-energy data. First two rows: Values found in the present analysis. Third row: Ref. 10, which is based on K_{l4} data alone. Fourth row: Values based on D-wave $\pi\pi$ scattering lengths and Zweig rule (Refs. 5 and 7(a)]. For error bars, see text.

	$10^3L_1^r$	$10^3L_2^r$	10^3L_3	$\bar{l}_1$	$\bar{l}_2$
No theor. error bars	0.65 ± 0.28	1.89 ± 0.26	-3.06 ± 0.92	-0.62 ± 0.94	6.28 ± 0.48
With theor. error bars	0.88 ± 0.47	1.61 ± 0.38	-3.62 ± 1.31	-0.81 ± 1.23	5.76 ± 0.71
K_{l4} alone (Ref. 10)	0.55	1.5	-2.8 ± 0.5	-0.52	5.55
$\pi\pi$ D-waves and Zweig rule [Refs. 5 and 7(a)]	0.9 ± 0.3	1.7 ± 0.7	-4.4 ± 2.5	-2.3 ± 3.7	6.0 ± 1.3

column of Table III).

While we were completing our analysis, we received a paper by Bijnens on this same topic.[10] Although notationally different from our form, we are in agreement with his calculations of the K_{l4} form factors. However, there are some differences in the phenomenology. In the order E^4 corrections, Bijnens uses a constant F_0, the pion decay constant in the limit of zero quark mass, rather than the physical pion decay constant, F_π. [For reasons which we do not understand he uses $F_0=82$ MeV instead of the value $F_0=87$ MeV estimated in Ref. 7(b).] The difference between the usage of F_0 and F_π is technically only a correction which is yet one order higher in the energy expansion; i.e., the difference is at order E^6. Nevertheless, the distinction makes a difference in the numerical values quoted. More important phenomenologically is the fact that Bijnens discusses K_{l4} reactions only. We have found the inclusion of $\pi\pi$ scattering to be a powerful phenomenological constraint. Thus in the end, our favored values of the low-energy constants differ somewhat from his—see the third row in Table IV, where we

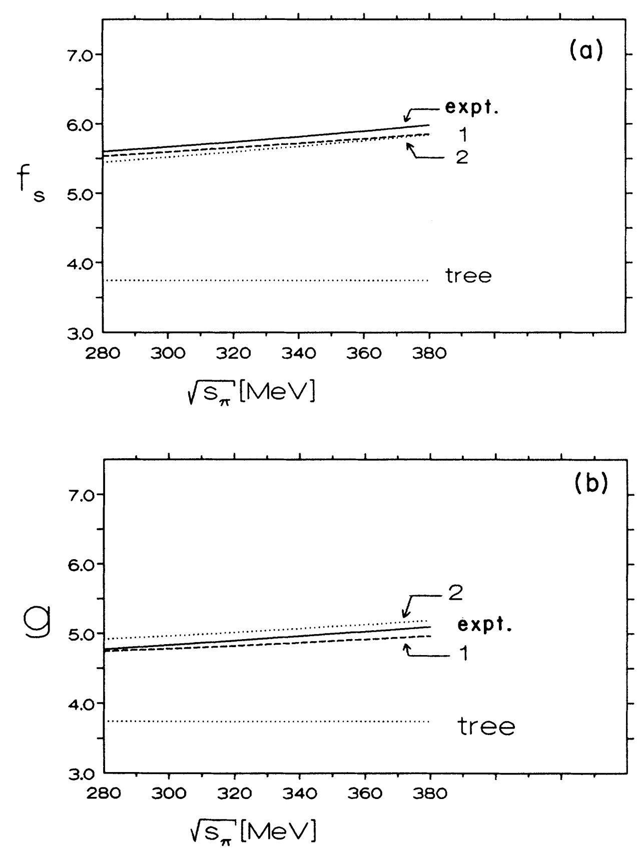

FIG. 3. The form factors $f_S(s_\pi)$ and $g(s_\pi)$ according to the chiral representation described in Sec. IV. Solid line: Experimental value. Curve 1: Central value according to the first row of Table IV. Curve 2: Same fit, with the additional large-N_c constraint $L_2=2L_1$.

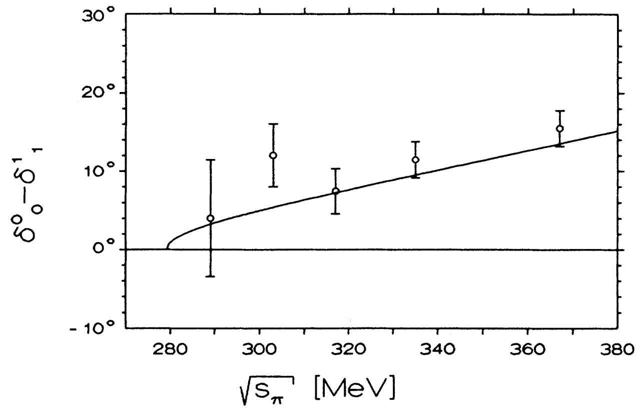

FIG. 4. The phase difference $\delta_0^0-\delta_1^1$. The data are from Ref. 11. The solid line displays the theoretical curve which corresponds to the first row of Table IV.

have also evaluated $\bar{l}_1$ and $\bar{l}_2$ corresponding to his values of L_1, L_2, and L_3. (Bijnens quotes the coupling constants at the scale $\mu=m_\rho$. We have reexpressed them at $\mu=m_\eta$.) The error quoted for L_3 is only due to the fit with data; no estimate for the next order term in the low-energy expansion was done. The values in the second row agree with his findings within the error bars.

VII. DISCUSSION

Chiral perturbation theory can describe very successfully the data of K_{l4} decays. Effects at order E^4 are important in this comparison. We have used this analysis for three purposes.

(i) The K_{l4} data plus chiral symmetry make predictions for λ_g and the $\pi\pi$ scattering lengths. These are given in Table III.

(ii) The K_{l4} data allow a test of the large-N_c predictions concerning chiral Lagrangians. This is shown in Eqs. (48)–(50).

(iii) The full set of K_{l4} and $\pi\pi$ data allows the best determination of the coefficients in the chiral Lagrangian. These are shown in Table IV, and represent the low-energy content of QCD.

The large-N_c rule works at the one standard deviation level for the combination $2L_1-L_2$. Overall, the data and the chiral analysis are in excellent agreement.

In the next generation of rare kaon decay experiments, there is the opportunity to improve the phenomenology of K_{l4}. The experimental uncertainty on G is still too large to provide a precise value for the large-N_c parameter $(L_2-2L_1)/L_3$. The observation of the other K_{l4} reactions with high statistics could provide a cleaner separation of the various isospin amplitudes. However, perhaps the most useful innovation would be to analyze the experimental data directly using the framework of chiral perturbation theory which we describe in this paper. Rather than making assumptions about the absence of P waves, D waves, etc., one could parametrize the data using the full chiral perturbation theory formulas, and directly decide the quality of the fit and the favored values of the low-energy constants. In addition, recall that K_{l4} decay is the only available source of clean information on $\pi\pi$ S-wave scattering near threshold. Future improvements in this area would also be welcome.

In conclusion, rare kaon decays provide a wealth of information on chiral perturbation theory, as well as constraints on fundamental interactions. It would be valuable to have a new study of K_{l4} decays in order to test the chiral and large-N_c predictions more exactly.

ACKNOWLEDGMENTS

We thank H. Leutwyler and J. L. Petersen for useful discussions. J.G. and C.R. profited much from discussions with J.-L. Basdevant, L. Rosselet, M. Sainio, H. Sazdjian, and J. Stern on various aspects of K_{l4} processes and are grateful to E. Hugentobler for providing a Monte Carlo integration program. J.F.D. thanks the Santa Fe QCD Study Group for hospitality during a portion of this work. The research of C.R. and J.G. was supported in part by Schweizerischer Nationalfonds. The research of J.F.D. and B.R.H. was supported in part by U.S. National Science Foundation.

APPENDIX

The loop integrals $J^r_{\pi\pi}, M^r_{\pi\pi}, \ldots$ which occur in the expression of the form factors F and G can be expressed in terms of the standard integral

$$\begin{aligned} J_{PQ}(z) &= -\frac{1}{16\pi^2}\int_0^1 \ln\frac{g(x;z)}{g(x;0)}dx \ , \\ g(x;z) &= m_P^2 - zx(1-x) - \Delta x \ , \\ \Delta &= m_P^2 - m_Q^2 \ . \end{aligned} \tag{A1}$$

In particular one has

$$J^r = \bar{J} - 2k, \quad K = \frac{\Delta}{2z}\bar{J}, \quad L = \frac{\Delta^2}{4z}\bar{J} \ , \tag{A2}$$

$$M^r = \frac{1}{12z}(z - 2m_P^2 - 2m_Q^2)\bar{J} + \frac{\Delta^2}{3z^2}\bar{\bar{J}} - \frac{k}{6} + \frac{1}{288\pi^2} \tag{A3}$$

with

$$\begin{aligned} k &= \frac{1}{32\pi^2}\left[m_P^2 \ln\frac{m_P^2}{\mu^2} - m_Q^2 \ln\frac{m_Q^2}{\mu^2}\right]\frac{1}{\Delta} \ , \\ \bar{\bar{J}}(z) &= \bar{J}(z) - z\bar{J}'(0) \ . \end{aligned} \tag{A4}$$

For $m_P = m_Q = m$,

$$\begin{aligned} \bar{J}(z) &= \frac{1}{16\pi^2}\left[\sigma \ln\frac{\sigma-1}{\sigma+1} + 2\right], \quad z<0 \ , \\ \sigma &= (1-4m^2/z)^{1/2} \ , \\ \bar{J}'(0) &= \frac{1}{96\pi^2}\frac{1}{m^2}, \quad k = \frac{1}{32\pi^2}\left[\ln\frac{m^2}{\mu^2} + 1\right] \ . \end{aligned} \tag{A5}$$

---

*Permanent address: Department of Physics and Astronomy, University of Massachusetts, Amherst, MA 01003.

[1]R. E. Marshak, Riazuddin, and C. P. Ryan, *Theory of Weak Interactions in Particle Physics* (Wiley-Interscience, New York, 1969).

[2]N. Cabibbo and A. Maksymovicz, Phys. Rev. **137**, B438 (1965); **168**, B1926(E) (1968); C. Kacser, P. Singer, and T. N. Truong, *ibid.* **137**, B1605 (1965).

[3]F. A. Berends, A. Donnachie, and G. C. Oades, Phys. Lett. **26B**, 109 (1967); Phys. Rev. **171**, 1457 (1968); A. Pais and S. B. Treiman, *ibid.* **168**, 1858 (1968).

[4]L. M. Chounet, J. M. Gaillard, and M. K. Gaillard, Phys. Rep. **4C**, 199 (1972); V. de Alfaro, S. Fubini, G. Furlan, and C. Rossetti, *Currents in Hadron Physics* (North-Holland, New York, 1973).

[5]J. Gasser and H. Leutwyler, Ann. Phys. (N.Y.) **158**, 142 (1984); Phys. Lett. **125B**, 321 (1983); **125B**, 325 (1983).

[6]S. Weinberg, Physica **A96**, 327 (1979); J. F. Donoghue, Proceedings of the International School of Physics with Low Energy Antiprotons, Erice, Italy, 1990 (unpublished).

[7]J. Gasser and H. Leutwyler, (a) Nucl. Phys. **B250**, 465 (1985); (b) **B250**, 517 (1985); (c) **B250**, 539 (1985).

[8]G. 't Hooft, Nucl. Phys. **B72**, 461 (1974).

[9]S. Weinberg, Phys. Rev. Lett. **17**, 336 (1966); **18**, 1178(E) (1967).

[10]J. Bijnens, Nucl. Phys. **B337**, 635 (1990).

[11]L. Rosselet *et al.*, Phys. Rev. D **15**, 574 (1977).

[12]J. Wess and B. Zumino, Phys. Lett. **37B**, 95 (1971); E. Witten, Nucl. Phys. **B223**, 422 (1980); **B223**, 433 (1980); N. K. Pak and P. Rossi, *ibid.* **B250**, 279 (1985).

[13]J. F. Donoghue, C. Ramirez, and G. Valencia, Phys. Rev. D **38**, 2195 (1988); **39**, 1947 (1989).

[14](a) G. Ecker, J. Gasser, A. Pich, and E. de Rafael, Nucl. Phys. **B321**, 311 (1989); (b) G. Ecker, J. Gasser, H. Leutwyler, A. Pich, and E. de Rafael, Phys. Lett. B **223**, 425 (1989); (c) J. F. Donoghue and B. R. Holstein, Phys. Rev. D **40**, 2378 (1989); (d) M. Praszalowicz and G. Valencia, Nucl. Phys. **B341**, 27 (1990); (e) D. Espriu, E. de Rafael, and J. Taron, *ibid.* **B345**, 22 (1990); (f) B. Holdom, J. Terning, and K. Verbeek, Phys. Lett. B **245**, 612 (1990).

[15]G. Veneziano, Nucl. Phys. **B117**, 519 (1976); E. Witten, *ibid.* **B156**, 269 (1979); **B160**, 57 (1979); Ann. Phys. (N.Y.) **128**, 363 (1980).

[16]T. N. Truong, Phys. Lett. **99B**, 154 (1981); in *Wandering in the Fields,* edited by K. Kawarabayashi and A. Ukawa (World Scientific, Singapore, 1987); Phys. Rev. Lett. **61**, 2526 (1988).

[17]M. M. Nagels *et al.,* Nucl. Phys. **B147**, 189 (1979).

[18]J.-L. Basdevant, C. D. Froggatt, and J. L. Petersen, Nucl. Phys. **B72**, 413 (1974); J.-L. Basdevant, P. Chapelle, C. Lopez, and M. Sigelle, *ibid.* **B98**, 285 (1975); C. D. Froggatt and J. L. Petersen, *ibid.* **B129**, 89 (1977).

[19]D. Morgan and G. Shaw, Nucl. Phys. **B10**, 261 (1968); J. L. Petersen, CERN Yellow Report No. CERN 77-04.

[20]N. H. Fuchs, H. Sazdjian, and J. Stern, Phys. Lett. B **238**, 380

(1990), and (unpublished); J. Stern (private communication).
[21]H. Leutwyler, in *Hadronic Matrix Elements and Weak Decay,* proceedings of the Ringberg Workshop, Ringberg Castle, West Germany, 1988, edited by A. J. Buras, J.-M. Gérard, and W. Huber [Nucl. Phys. B (Proc. Suppl.) **7A**, 42 (1989)].
[22]A. Pich, talk given at the Workshop on Rare Decays of Light Mesons, Gif-sur-Yvette, France, 1990 (unpublished).